Journal of Alloys and Compounds 509 (2011) 8788–8793

Contents lists available at ScienceDirect

Journal of Alloys and Compounds

journal homepage: www.elsevier.com/locate/jallcom

Color-conversion and photoluminescence properties of $Ba_2MgW(Mo)O_6$:Eu phosphor

Huaiyong Li[a], Hyun Kyoung Yang[a], Byung Kee Moon[a], Byung Chun Choi[a], Jung Hyun Jeong[a,*], Kiwan Jang[b], Ho Sueb Lee[b], Soung Soo Yi[c]

[a] Department of Physics, Pukyong National University, Busan 608-737, Republic of Korea
[b] Department of Physics, Changwon National University, Changwon 641-773, Republic of Korea
[c] Department of Electronic Material Engineering, Silla University, Busan 617-736, Republic of Korea

ARTICLE INFO

Article history:
Received 8 March 2011
Received in revised form 14 June 2011
Accepted 16 June 2011
Available online 22 June 2011

Keywords:
Phosphors
Inorganic materials
Optical properties
Luminescence

ABSTRACT

Compounds B_2AXO_6:Eu (B = Ba, Sr; A = Ca; and X = W, Mo) have recently been investigated and suggested to be color-conversion phosphor for WLED devices. In this work, we investigated the photoluminescence properties of the analogues Ba_2MgXO_6:Eu (X = W and Mo) and the energy transfer from $W(Mo)O_6$ groups to Eu^{3+} ions within the phosphors. The phase structure, UV–vis diffuse reflectance spectrum, photoluminescence properties and decay of $Ba_2MgW_{(1-x)}Mo_xO_6$:Eu were studied as a function of the W/Mo ratio. It was found that these phosphors showed excellent color-conversion capability from near-UV to orange–red light. The color-conversion process was considered to be performed by energy transferring from MoO_6 groups to doped Eu^{3+} ions. The $MoO_6 \rightarrow Eu^{3+}$ energy transfer efficiency could be greatly enhanced by partial substitution of Mo by W. The structure and photoluminescence properties of $Ba_2AW_{0.5}Mo_{0.5}O_6$:Eu (A = Ca and Mg, respectively) compounds were also investigated to reveal the effect of the Eu^{3+} ion coordination environment on its photoluminescence properties.

1. Introduction

White light emitting diode (WLED) devices based on near-UV/blue LED and inorganic phosphors have attracted great interest in recent years due to their significant advantageous, such as energy-conservation, high efficiency and compact [1–3]. In these devices, the inorganic phosphors are used to absorb the near-UV/blue light emitted from LED, and then convert the energy into red, green and blue (RGB) light emission, thus to absorb near-UV/blue light is very important for a color-conversion phosphor [4–6]. The widely used commercial WLED, which consists of a blue LED and a yellow phosphor ($Y_3Al_5O_{12}$:Ce^{3+}), has high luminous efficiency, while poor color rendering index (CRI) due to the weak red light emission [7,8]. In order to improve the performance of $Y_3Al_5O_{12}$:Ce^{3+} phosphor, a great amount of investigations has been performed [9–18]. On the other hand, it was also pointed out that WLED devices with high CRI and luminous can be created from near-UV/blue LED and RGB tricolor phosphors [1]. Therefore continued efforts are devoted to the investigation of near-UV/blue LED excited RGB phosphors, especially red phosphors [19–32]. As the most widely used red light emitting ion, Eu^{3+} ions are excellent in many aspects, and consequently great many Eu^{3+} activated phosphors have been investigated [33]. The proposed phosphors can be basically divided into two groups according to the excitation channels. For one group, the Eu^{3+} ion is excited directly through the *f–f* transition [34–38]; for the other group, sensitizers are introduced to absorb the excitation light and sensitize the doped Eu^{3+} ion [39–44]. Since the Eu^{3+} ion *f–f* transition is spin and parity forbidden, exciting into a sensitizer other than Eu^{3+} ion might be a promise way to increase the energy absorption efficiency. In other words, searching for suitable sensitizers for Eu^{3+} is of applicative importance.

It has been reported that MoO_4–MoO_6 groups can absorb near-UV and violet light efficiently [45]. Recently, host sensitized, Eu^{3+} ion-activated B_2AMoO_6:Eu (B = Ba, Sr; A = Ca) phosphors were investigated as color-conversion phosphors for WLED devices [39–42,44]. According to the investigations, the near-UV excitation energy can be absorbed by the MoO_6 groups in the B_2CaMoO_6:Eu systems, and then transferred to the doped Eu^{3+} ions, resulting in intensive orange–red light emission [39–42]. Furthermore, it was also found that partial substituting of the MoO_6 groups with WO_6 groups did not change the MoO_6 excitation band position significantly, but enhanced the photoluminescence (PL) intensity greatly [41,42]. We noticed that the cubic double-perovskite structure could also be adopted by Ba_2MgMoO_6 and Ba_2MgWO_6 compounds [46], while these compounds have not been investigated as the host lattice, as well as the sensitizer of Eu^{3+} ions. On the other side, when doped into the B_2AMoO_6 lattice, Eu^{3+} ion was considered

* Corresponding author. Tel.: +82 51 629 5564; fax: +82 51 629 5549.
E-mail address: jhjeong@pknu.ac.kr (J.H. Jeong).

0925-8388/$ – see front matter © 2011 Elsevier B.V. All rights reserved.
doi:10.1016/j.jallcom.2011.06.073

to preferably occupy A-site, namely, Ca^{2+}-site in Ba_2CaMoO_6 [41], and Mg^{2+}-site in Ba_2CaMoO_6. Since the ionic radius of Mg^{2+} is much smaller than that of Ca^{2+}, it is reasonable to expect that the coordination environment of Mg^{2+} might significantly differ from that of Ca^{2+}. The influence of this variation on the PL properties of Eu^{3+} ions has not been revealed.

In the study presented here, the color-conversion and PL properties of Eu^{3+} ion activated $Ba_2MgW_{(1-x)}Mo_xO_6$ have been investigated as a function of the W/Mo ratio. The energy immigration among MoO_6 groups and energy transfer from MoO_6 groups to doped Eu^{3+} ions were discussed with an existed theory. In order to evaluate the effect of the coordination environment of Eu^{3+} ions on their PL properties, we also synthesized a series of compounds with varied Mg/Ca ratios, namely $Ba_2Mg_{(1-y)}Ca_yW_{0.5}Mo_{0.5}O_6$:Eu, and studied their structure and PL properties.

2. Experimental

All the compounds were synthesized by using a high-temperature solid-state reaction. The start materials $BaCO_3$ (99+%), $CaCO_3$ (99+%), MgO (99.99%), WO_3 (99.0%), MoO_3 (99.5%) and Eu_2O_3 (99.99%) obtained from Sigma–Aldrich were weighted out according to stoichiometric ratio, and then mixed and ground in an agate mortar. The mixtures were firstly preheated at 850 °C for 24 h, and then calcined at 1175 °C and 1200 °C for 20 and 12 h, respectively [47]. After each heating process, the samples were ground to increase the homogeneity.

The phase structure of the powders was examined by using the X-ray diffraction (XRD) measurement, which was carried out on a Philips X'Pert MPD X-ray diffraction system at 40 kV and 30 mA. The diffraction patterns were scanned over an angular range of 15–75° (2θ). The UV–vis diffuse reflectance (DR) spectra were measured on a JASCO V-670 spectrophotometer from 200 to 600 nm. The PL excitation and emission spectra were recorded on a PTI fluorescence spectrophotometer equipped with a 60 W Xe-arc lamp. The decay data were collected with a phosphorimeter attachment to the fluorescence spectrophotometer with a 25 W Xe-flash lamp. All the measurements were performed at room temperature in air.

3. Results and discussion

3.1. Ba_2MgMoO_6–Ba_2MgWO_6 series

The XRD patterns shown in Fig. 1 indicate that all the compositions crystallize in the same phase, which can be indexed to the cubic double perovskite structure. According to the reported structure information [46], Ba_2MgWO_6 cell belongs to the $Fm\bar{3}m$ space group (no. 225) [48]. In the cell, Ba^{2+} ions, which have large ionic radius, reside in the $8c$ (1/4, 1/4, 1/4) Wyckoff sites, while Mg^{2+} and W^{6+} ions with relatively small radii reside in the $4a$ (0, 0, 0) and

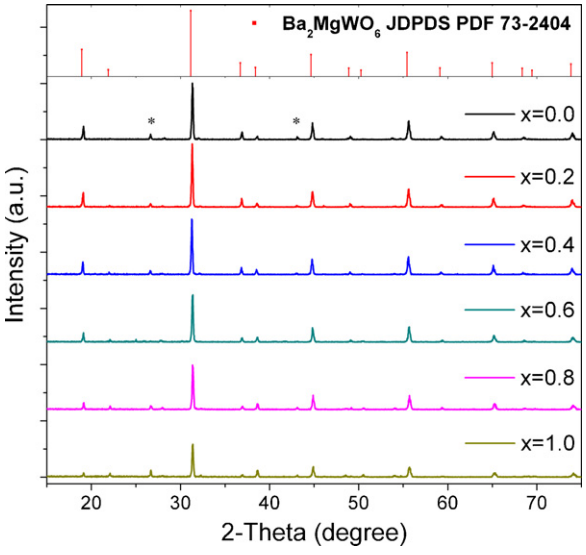

Fig. 1. XRD patterns of $Ba_2MgW_{(1-x)}Mo_xO_6$:Eu, along with the JCPDS card of Ba_2MgWO_6. Symbol * indicates the diffraction peaks due to $BaW(Mo)O_4$ impurity.

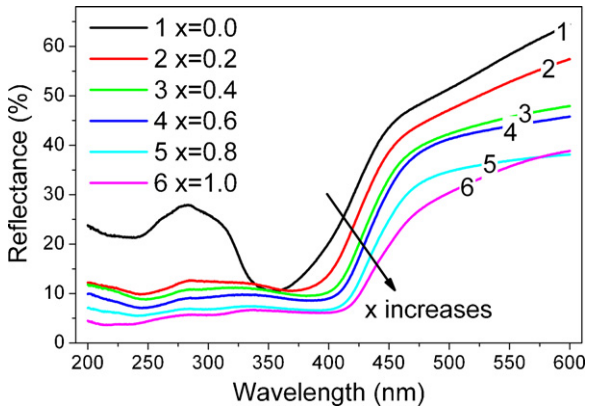

Fig. 2. UV–vis DR spectra of $Ba_2MgW_{(1-x)}$ Mo_xO_6:Eu.

$4b$ (1/2, 0, 0) sites, respectively. Both Mg^{2+} and W^{6+} ions are 6-fold coordinated to oxygen forming MgO_6 and WO_6 octahedra. These octahedra appear alternately in the cell and are connected with each other by sharing vertex oxygen [46]. In the double perovskite structure, the $8c$ site can be also occupied by Sr^{2+}, the $4a$ site by Mo^{6+}, and the $4b$ by Ca^{2+}, Zn^{2+}, etc. The double perovskite structure might be distorted from cubic depending on the ionic radii of the ions on 8c, 4a and 4b sites. In our case, the W on $4a$ sites was substituted by Mo gradually, and it was found that both compounds, namely Ba_2MgWO_6 (BMWO) and Ba_2MgMoO_6 (BMMO), have the same cubic structure, and furthermore they can form solid solution in all expected ratios. Owing to the ionic radius of Mo^{6+} ions (0.59 Å) is slightly larger than that of W^{6+} ions (0.60 Å) [49], the lattice constants vary from $a = 8.0704$ of BMWO to $a = 8.0566$ of BMMO.

Fig. 2 shows the DR spectra of the BMWO– BMMO samples. As expected, these samples have strong absorption of UV and near-UV light. The absorption is ascribed to the optical excitation of electrons from the valence band, which is mainly of O-2p character, to the conductive band, which is mainly of Mo-4d or W-5d character [41]. It is observed that the absorption edge of the BMWO–BMMO series red shifts gradually with the increasing of the Mo-content, which indicates the variation of the band gap with the element substitution. As well-known that the absorption coefficient (α) of a semiconductor oxide and its band gap energy E_g are related through $(\alpha h\upsilon)^2 \propto h\upsilon$, in which h is the Planck constant, υ is the frequency of the light. By plotting $(\alpha h\upsilon)^2 \sim h\upsilon$ derived from the DR spectra the band gap energy E_g of BMWO–BMMO compounds were estimated and listed in Table 1.

The PL excitation, emission spectra and the CIE chromatic coordinates (x, y) of the emission spectra are shown in Fig. 3. The PL excitation spectra shown in Fig. 3a were recorded by monitoring Eu^{3+} ion characteristic emission at 598 nm. While not only the excitation of Eu^{3+} ions $^7F_0 \rightarrow {}^5L_6$ transition centered at 399.5 presented in all the spectra, but also a broad-band excitation appeared. The band centered at 314 nm in BMWO is ascribed to the electronic excitation of O(2p) → W(5d) within WO_6 groups [50], and

Table 1
Band gap energy (E_g) in eV, CIE coordinates (x, y), and lifetime (τ) in ms of $Ba_2MgW_{(1-x)}Mo_xO_6$:Eu phosphors.

Composition	E_g (eV)	(x, y)	τ (ms)
$x = 1.0$	2.11	(0.648, 0.351)	1.89(2)
$x = 0.8$	2.29	(0.645, 0.354)	2.41(2)
$x = 0.6$	2.41	(0.645, 0.354)	2.30(2)
$x = 0.4$	2.44	(0.643, 0.356)	2.52(2)
$x = 0.2$	2.46	(0.632, 0.366)	2.64(3)
$x = 0.0$	2.47	(0.618, 0.379)	3.22(4)

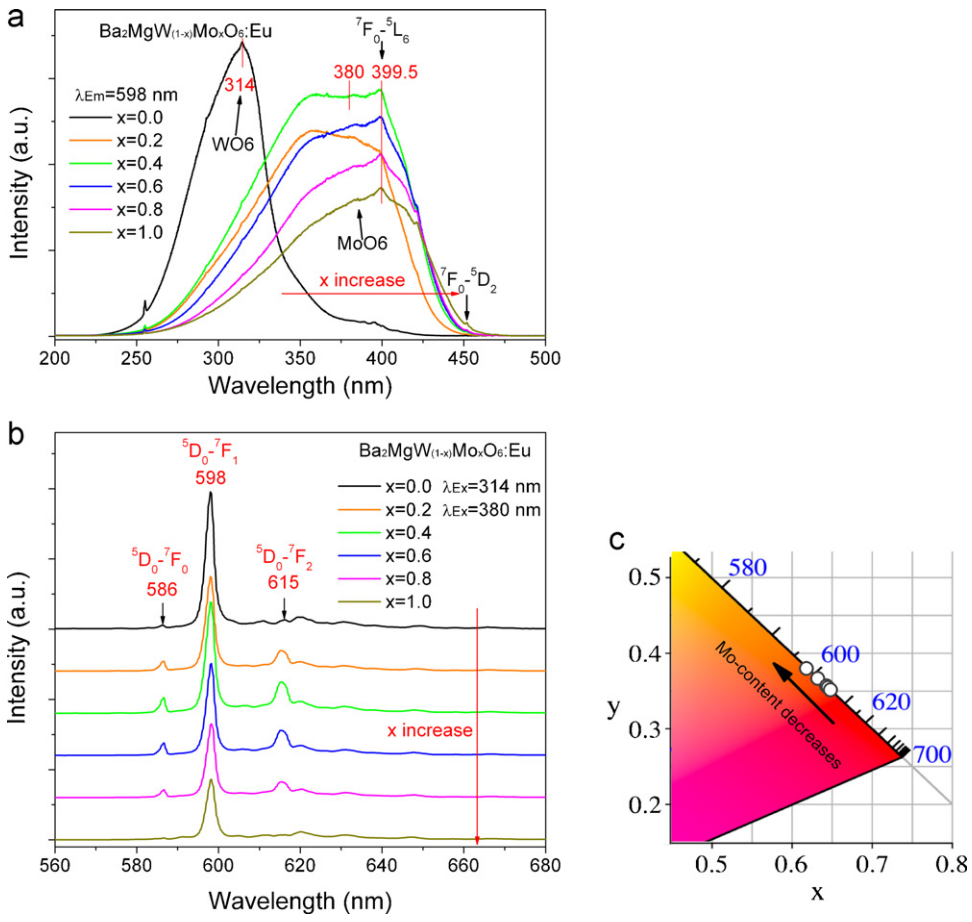

Fig. 3. Photoluminescence (a) excitation, (b) emission spectra, and (c) chromatic coordinate (x, y) of the emission of $Ba_2MgW_{(1-x)}Mo_xO_6$:Eu series. λ_{Em} and λ_{Ex} are the emission and excitation wavelength, respectively.

that centered at 400 nm in BMMO is due to the electron transition from O(2p) to Mo(4d) orbitals in MoO_6 groups [45]. In the cases of the solid solutions BMWO–BMMO, the bands are similar to the MoO_6 excitation band within BMMO, and the excitation of WO_6 groups cannot be identified. This differs from the results shown in $Ba_2CaW_{(1-x)}Mo_xO_6$:Eu and $Y_6W_{(1-x)}Mo_xO_{12}$:Eu series. The presence of the host lattice excitation bands indicates that there is energy transfer from host lattices to doped Eu^{3+} ions in these compounds. And furthermore, from the spectra one might noticed that for 598 nm emission, the excitations of the host lattices (WO_6 and MoO_6) are far more efficient than that of the Eu^{3+} ion f–f transitions. This is due to the fact that the f–f transitions of Eu^{3+} ions are intraconfigurational, and therefore they are spin and parity forbidden, whereas the transitions within WO_6 and MoO_6 groups are of charge transfer type and allowed. In Fig. 3a it is also observed that the edge of the excitation band red shifts with the increasing of Mo content, which is consistent with the DR spectra.

As regards the PL emission spectra (see Fig. 3b), they are obtained by exciting the host lattices at 314 nm for BMWO, and at 380 nm for Mo-contained compounds. All the PL emission spectra have similar profile, containing several sharp peaks centered at 586, 598 and 615 nm, which are due to the f–f transition of $^5D_0 \rightarrow {}^7F_0$, $^5D_0 \rightarrow {}^7F_1$, and $^5D_0 \rightarrow {}^7F_2$, respectively. Although the emission intensity varies with the Mo content, the $^5D_0 \rightarrow {}^7F_1$ emission is dominated in all the spectra. The calculated CIE chromatic coordinates (x, y) of the emissions indicate that when Mo is gradually substituted by W, the emission color shifts slightly from red to orange–red (see Fig. 3c). This character originates from the symmetry of the sites Eu^{3+} ions occupied. According to the structure refinement, Mg^{2+} ions and therefore Eu^{3+} ions in the cell take the 4*b* Wyckoff sites with the O_h point group symmetry, under which the $^7F_0$, $^7F_1$ and $^7F_2$ energy levels will be of 1-, 1- and 2-fold splitting, respectively. If the parity selective rule is strictly obeyed, only $^5D_0 \rightarrow {}^7F_1$ emission can be observed. In our case, all the emissions of $^5D_0 \rightarrow {}^7F_{0,1,2}$ are observed despite the $^5D_0$–$^7F_1$ emission is dominated. This indicates that in these lattices the 4*b* sites deviate from the O_h point symmetry. To exam the deviation degree, the R/O ratio, which is defined as the integral intensity ratio of $^5D_0 \rightarrow {}^7F_2$ to $^5D_0 \rightarrow {}^7F_1$ emissions, is commonly used as a measurement [51]. The R/O ratios plotted in Fig. 4 clearly shows that the R/O ratios of the

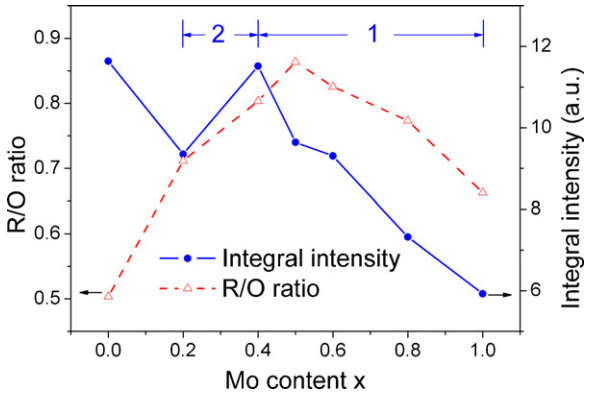

Fig. 4. Variation of the integral intensity and R/O ratio of the $Ba_2MgW_{(1-x)}Mo_xO_6$:Eu emission spectra with the Mo content x.

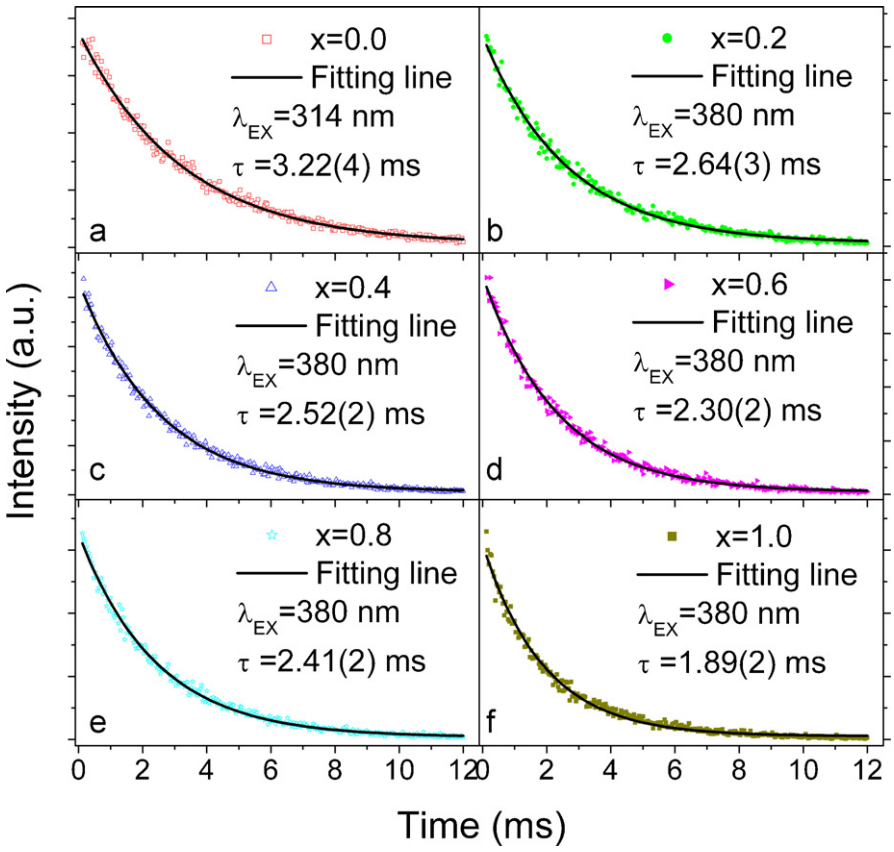

Fig. 5. Photoluminescence decay data of $Ba_2MgW_{(1-x)}Mo_xO_6$:Eu. λ_{Ex} is the excitation wavelength, and the emission wavelength is 598 nm for all the samples. τ is the lifetime.

parent compounds BMWO and BMMO are relatively small, when the Mo-content approaches 0.5, the R/O ratio reaches its maximum, which implies the distortion of the 4*b* site arrives at its peak.

We also calculated the integral intensity of each emission in the range of 500–700 nm and plotted them versus the Mo content *x* in Fig. 4. As indicated that BMWO:Eu^{3+} shows the strongest emission, while BMMO:Eu^{3+} shows the weakest one. This suggests that the energy transfer efficiency of $WO_6 \rightarrow Eu^{3+}$ is higher than that of $MoO_6 \rightarrow Eu^{3+}$. The most interesting phenomenon shown in Fig. 4 is the variation of the integral intensity of the Mo-contained compounds. In these compounds, the doped Eu^{3+} ions are sensitized by MoO_6 groups, and therefore the changing of the emission intensity reflects the variation of the $MoO_6 \rightarrow Eu^{3+}$ energy transfer process. According to the tendency, the curve can be simply separated into two stages (stages 1 and 2 as shown in Fig. 4): in stage 1, when the Mo-content decreasing from 1.0 to 0.4, the emission increases gradually; in stage 2, when *x* decreases further from 0.4 to 0.2, the emission decreases simultaneously. This phenomenon was similarly observed in the $Ba_2CaW_{(1-x)}Mo_xO_6$:Eu and $Y_6W_{(1-x)}Mo_xO_{12}$:Eu systems [41,43]. According to Ye et al. [41], and Wiegel and Blasse [45], there are at least two competitive processes undergoing after the MoO_6 groups are excited. During one of the processes the excitation energy immigrates among the MoO_6 groups, and finally nonradiatively dissipated. In the other process the energy is transferred from MoO_6 groups to Eu^{3+} ions, which finally generates the emission. In stage 1, the energy immigration among MoO_6 groups is supposed to dominate, and therefore the more MoO_6 groups exists in the system, the more energy is dissipated among the MoO_6 groups, and the less energy can arrive at Eu^{3+} ions. While in stage 2, since the MoO_6 concentration is lower than the critical value, the energy immigration among MoO_6 groups is not efficient anymore, consequently, the emission of Eu^{3+} is proportional to the MoO_6 concentration.

The decay data of BMWO–BMMO compounds are shown in Fig. 5. All the data can be well fitted by a monoexponential decay function $I_t = I_0 \exp(-t/\tau)$, where I_t and I_0 are the intensity at time *t* and $t = 0$, respectively, τ is the decay lifetime. The calculated lifetimes are summarized in Table 1. It is illustrated that lifetime of the excitation state increases gradually from 1.89 ms to 2.64 ms with the decreasing of Mo-content.

3.2. $Ba_2MgMo_{0.5}W_{0.5}O_6$–$Ba_2CaMo_{0.5}W_{0.5}O_6$ series

In order to evaluate the dependence of the Eu^{3+} ions PL properties on their coordination environment, we made an attempt to synthesize phosphor of compositions $Ba_2Mg_{(1-y)}Ca_yW_{0.5}Mo_{0.5}O_6$:Eu ($y = 0.0, 0.25, 0.50, 0.75, 1.0$). Whereas from the XRD patterns shown in Fig. 6 one can find that the result is not satisfied because the $Ba_2MgW_{0.5}Mo_{0.5}O_6$ (BMXO) and $Ba_2CaW_{0.5}Mo_{0.5}O_6$ (BCXO) do not form solid solution at desired ratios. This might due to the fact that the ionic radii of Mg^{2+} and Ca^{2+} ions differ from each other greatly: the ionic radius of the 6-folded Mg^{2+} was determined to be 0.72 Å, while that of the Ca^{2+} is 1.00 Å [49], as a consequence, the cell parameter of BMXO ($a = 8.0614$ Å, calculated from the XRD pattern shown in Fig. 6) is obviously smaller than that of the BCXO ($a = 8.3517$ Å). Accordingly, we merely checked the PL properties of compounds BMXO and BCXO. Fig. 7 indicated that the PL excitation and emission spectra of the two compounds are similar to each other in most respects. Both PL excitation spectra consist of a strong excitation band of the host lattice and several very weak Eu^{3+} characteristic excitation peaks. The PL emission spectra are dominated respectively by the line-emission centered at 598.50

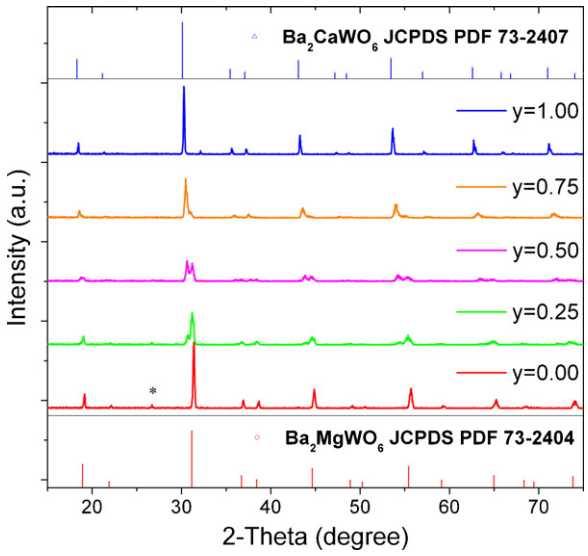

Fig. 6. XRD patterns of $Ba_2Mg_{(1-y)}Ca_yW_{0.5}Mo_{0.5}$:Eu series and the JCPDS cards of Ba_2CaWO_6 and Ba_2MgWO_6. Symbol * indicates the diffraction peaks due to $BaW(Mo)O_4$ impurity.

and 596.75 nm, which are due to the $^5D_0 \rightarrow {}^7F_1$ transition of Eu^{3+} ions. The red shift of the $^5D_0 \rightarrow {}^7F_1$ emission might be rose from the variation of the chemical environmental from Ca^{2+} to Mg^{2+}. Consequently, the chromatic coordinate (x, y) of the emission shifts slightly from (0.634, 0.365) of BCXO to (0.641, 0.358) of BMXO. The most significant difference of the two spectra is the PL intensity. The integral intensity of BMXO is 9.64×10^6, which is stronger than that of BCXO (2.32×10^6) by 4.15 times. From the viewpoint of luminescence efficiency, the BMXO is superior to the BCXO. When noticed the pure Ca-contained cubic phase is easier to obtain than the Mg-contained cubic phase. As shown in Figs. 1 and 6, even the reactants are sustained at high-temperature for 32 h, there is still some $BaMoO_4$ and/or $BaWO_4$ impure (indicated as * in Figs. 1 and 6) existed. This situation does not happen on the Ca-contained compounds. Although it was reported that the pure cubic phase can be synthesized [47], it need more sustain time, which is not beneficial to the energy-conservation.

As a red color-conversion phosphor for WLED, the candidate is expected to absorb near-UV/blue light (wavelength ranging from 370 to 450 nm), and then to convert the excitation energy into red light emission. The existed red-emitting phosphors, such as Y_2O_2S:Eu, show excellent red emission under UV excitation, while the excitation efficiency declines dramatically when the

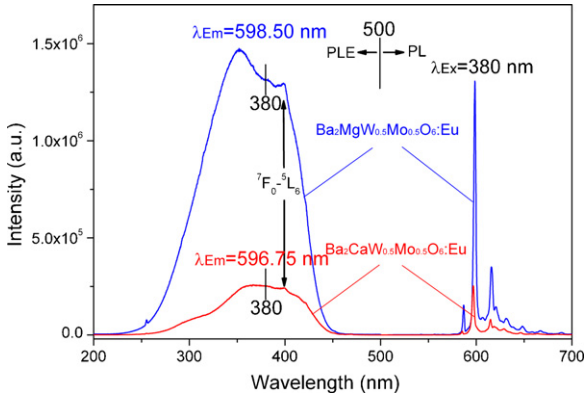

Fig. 7. PL excitation and PL emission of $Ba_2MgW_{0.5}Mo_{0.5}$:Eu and $Ba_2CaW_{0.5}Mo_{0.5}$:Eu. λ_{Em} and λ_{Ex} are the emission and excitation wavelength, respectively.

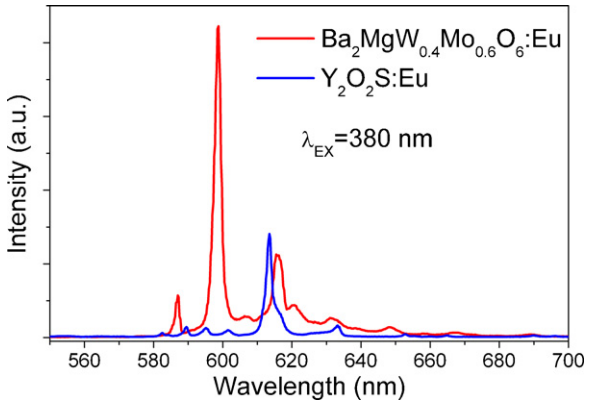

Fig. 8. Emission spectra of $Ba_2MgW_{0.4}Mo_{0.6}$:Eu and commercial phosphor $Y_2O_2S:Eu^{3+}$. Both phosphors were under 380 nm excitation.

excitation light shifts from UV to near-UV region. Comparatively, BMWO–BMMO series have strong absorption in near-UV region. The absorbed excitation energy can then be transferred from host lattices to doped Eu^{3+} ions, resulting in orange–red emission. From the spectra shown in Fig. 8 one can find that the near-UV excitation efficiency of $Ba_2MgW_{0.4}Mo_{0.6}O_6$:Eu is significantly higher than that of Y_2O_2S:Eu. The drawback of BMWO–BMMO series is their emissions, which are dominated by orange–red emission instead of red emission.

4. Conclusions

The phase structure, color-conversion and photoluminescence properties of two series of compounds Ba_2AXO_6:Eu, A = Mg, $X = W_{(1-x)}Mo_x$ and $A = Mg_{(1-y)}Ca_y$, $X = W_{0.5}Mo_{0.5}$ have been respectively investigated. BMWO and BMMO can form solid solution at any desired ratio, while BCXO and BMXO do not at all. As $Ba_2CaW_{(1-x)}Mo_xO_6$:Eu series, the $Ba_2MgW_{(1-x)}Mo_xO_6$:Eu series show excellent color-conversion capability. The energy transfer from MoO_6 groups to Eu^{3+} ions was considered to play a decisive role in the color-conversion process. The substitution of Mo by W greatly benefits the energy transfer efficiency, and therefore increases the luminescence intensity, but changes the chromatic coordinate of the emission from red to orange–red. The environment of the site Eu^{3+} ions occupied also affects the photoluminescence properties significantly and the luminescence intensity can be greatly enhanced by replacing Ca with Mg. BMWO–BMMO phosphors are superior to the commercial red phosphor Y_2O_2S:Eu in the PL intensity.

Acknowledgements

This study was supported by the Korea Research Foundation Grant funded by the Korean Government (NRF-2010-0029634, no. 2010-0029885) and also partially by National Core Research Center Program through the NRF of Korea funded by the Ministry of Education, Science and Technology (2010-0001-226).

References

[1] E.F. Schubert, J.K. Kim, Science 308 (2005) 1274–1278.
[2] H. Luo, J.K. Kim, E.F. Schubert, J. Cho, C. Sone, Y. Park, Appl. Phys. Lett. 86 (2005) 1–3.
[3] A. Bergh, G. Craford, A. Duggal, R. Haitz, Phys. Today 54 (2001) 42–47.
[4] H.A. Höppe, Angew. Chem. Int. Ed. 48 (2009) 3572–3582.
[5] C. Feldmann, T. Jüstel, C.R. Ronda, P.J. Schmidt, Adv. Funct. Mater. 13 (2003) 511–516.
[6] T. Jüstel, H. Nikol, C. Ronda, Angew. Chem. Int. Ed. 37 (1998) 3084–3103.
[7] T. Justel, in: C. Ronda (Ed.), Luminescence From Theory to Applications, Wiley-VCH Verlag GmbH & Co. KGaA, Weinheim, 2008, pp. 179–190.

[8] J. Silver, R. Withnall, in: A. Kitai (Ed.), Luminescent Materials and Applications, John Wiley & Sons, Ltd., Chichester, 2008, pp. 75–109.
[9] Y.-T. Nien, K.-M. Chen, I.-G. Chen, J. Am. Ceram. Soc. 93 (2010) 1688–1691.
[10] W.-H. Chao, R.-J. Wu, T.-B. Wu, J. Alloys Compd. 506 (2010) 98–102.
[11] N. Jia, X. Zhang, W. He, W. Hu, X. Meng, Y. Du, J. Jiang, Y. Du, J. Alloys Compd. 509 (2011) 1848–1853.
[12] X. Su, K. Zhang, Q. Liu, H. Zhong, Y. Shi, Y. Pan, ACS Comb. Sci. 13 (2010) 79–83.
[13] X. Jiang, Y. Wang, C. Pan, J. Alloys Compd. 509 (2011) L1137.
[14] A.B. Munoz-Garcia, L. Seijo, J. Phys. Chem. A 115 (2011) 815–823.
[15] G. Liu, J. Li, S. Guo, X. Ning, Y. Chen, J. Alloys Compd. 509 (2011) L2213.
[16] D. Amans, C. Malaterre, M. Diouf, C. Mancini, F. Chaput, G. Ledoux, G. Breton, Y. Guillin, C. Dujardin, K. Masenelli-Varlot, P. Perriat, J. Phys. Chem. C 115 (2011) 5131–5139.
[17] Q. Shao, H. Li, Y. Dong, J. Jiang, C. Liang, J. He, J. Alloys Compd. 498 (2010) 199–202.
[18] C.W. Won, H.H. Nersisyan, H.I. Won, J.H. Lee, K.H. Lee, J. Alloys Compd. 509 (2011) 2621–2626.
[19] M. Krings, G. Montana, R. Dronskowski, C. Wickleder, Chem. Mater. 23 (2011) 1694–1699.
[20] Z. Cui, R. Ye, D. Deng, Y. Hua, S. Zhao, G. Jia, C. Li, S. Xu, J. Alloys Compd. 509 (2011) 3553–3558.
[21] B.K. Grandhe, V.R. Bandi, K. Jang, S.-S. Kim, D.-S. Shin, Y.-I. Lee, J.-M. Lim, T. Song, J. Alloys Compd. 509 (2011) 7937–7942.
[22] Z.-H. Ju, R.-P. Wei, J.-X. Ma, C.-R. Pang, W.-S. Liu, J. Alloys Compd. 507 (2010) 133–136.
[23] C. Duan, Z. Zhang, S. Rosler, S. Rosler, A. Delsing, J. Zhao, H.T. Hintzen, Chem. Mater. 23 (2011) 1851–1861.
[24] Y. Liu, W. Zhuang, Y. Hu, W. Gao, J. Hao, J. Alloys Compd. 504 (2010) 488–492.
[25] W. Ma, Z. Shi, R. Wang, J. Alloys Compd. 503 (2010) 118–121.
[26] T. Suehiro, N. Hirosaki, R.-J. Xie, ACS Appl. Mater. Interfaces 3 (2011) 811–816.
[27] Z. Sun, Q. Zhang, Y. Li, H. Wang, J. Alloys Compd. 506 (2010) 338–342.
[28] X. Yan, W. Li, K. Sun, J. Alloys Compd. 508 (2010) 475–479.
[29] C.C. Lin, R.-S. Liu, J. Phys. Chem. Lett. 2 (2011) 1268–1277.
[30] S.-s. Yao, L.-h. Xue, Y.-w. Yan, J. Alloys Compd. 509 (2011) 1870–1873.
[31] R. Zhang, X. Wang, J. Alloys Compd. 509 (2011) 1197–1200.
[32] X. Zhang, M. Gong, J. Alloys Compd. 509 (2011) 2850–2855.
[33] S. Ye, F. Xiao, Y.X. Pan, Y.Y. Ma, Q.Y. Zhang, Mater. Sci. Eng. R. 71 (2010) 1–34.
[34] S. Neeraj, N. Kijima, A.K. Cheetham, Chem. Phys. Lett. 387 (2004) 2–6.
[35] V. Sivakumar, U.V. Varadaraju, J. Solid State Chem. 181 (2008) 3344–3351.
[36] H. Li, S. Zhang, S. Zhou, X. Cao, Y. Zheng, J. Phys. Chem. C 113 (2009) 13115–13120.
[37] Z. Wang, H. Liang, M. Gong, Q. Su, J. Alloys Compd. 432 (2007) 308–312.
[38] C. Guo, F. Gao, L. Liang, B.C. Choi, J.-H. Jeong, J. Alloys Compd. 479 (2009) 607–612.
[39] V. Sivakumar, U.V. Varadaraju, J. Electrochem. Soc. 154 (2007) J28–J31.
[40] V. Sivakumar, U.V. Varadaraju, Electrochem. Solid State Lett. 9 (2006) H35–H38.
[41] S. Ye, C.H. Wang, Z.S. Liu, J. Lu, X.P. Jing, Appl. Phys. B 91 (2008) 551–557.
[42] S. Ye, C.H. Wang, X.P. Jing, J. Electrochem. Soc. 155 (2008) J148–J151.
[43] H. Li, H.K. Yang, B.K. Moon, B.C. Choi, J.H. Jeong, K. Jang, H.S. Lee, S.S. Yi, J. Mater. Chem. 21 (2011) 4531–4537.
[44] X. Zhang, Z. Li, H. Zhang, S. Ouyang, Z. Zou, J. Alloys Compd. 469 (2009) L66.
[45] M. Wiegel, G. Blasse, J. Solid State Chem. 99 (1992) 388–394.
[46] V.S. Filip'ev, G.E. Shatalova, E.G. Fesenko, Kristallografiya 19 (1974) 386–387.
[47] S.J. Patwe, S.N. Achary, M.D. Mathews, A.K. Tyagi, J. Alloys Compd. 390 (2005) 100–105.
[48] T. Hahn (Ed.), Int. Tables Crystallogr. Vol. A, Springer, Dordrecht, 2005, pp. 688–691.
[49] R. Shannon, Acta Crystallogr. A 32 (1976) 751–767.
[50] A.B.V. Oosterhout, Phys. Stat. Sol. (a) 41 (1977) 607–617.
[51] G. Blasse, B.C. Grabmaier, Luminescent Materials, Springer-Verlag, Berlin Heidelberg, 1994.